Journal of Physics: Conference Series

Design of Magnetic Charged Particle Lens Using Analytical Potential Formula

To cite this article: A H Al-Batat *et al* 2018 *J. Phys.: Conf. Ser.* **1003** 012111

Design of Magnetic Charged Particle Lens Using Analytical Potential Formula

A H Al-Batat [1], M J Yaseen [1], S R Abbas [1], M S Al-Amshani [1] and **H S Hasan [2]**

[1]Department of Physics, College of Education, Mustansiriyah University, P.O.Box:46219, Baghdad, Iraq.

[2]Department of Physiology and Medical Physics, College of Medicine, Al-Nahrain University, P.O. Box: 70044, Kadhimiya, Baghdad, Iraq.

Abstract: In the current research was to benefit from the potential of the two cylindrical electric lenses to be used in the product a mathematical model from which, one can determine the magnetic field distribution of the charged particle objective lens. With aid of simulink in matlab environment, some simulink models have been building to determine the distribution of the target function and their related axial functions along the optical axis of the charged particle lens. The present study showed that the physical parameters (i.e., the maximum value, B_{max}, and the half width W of the field distribution) and the objective properties of the charged particle lens have been affected by varying the main geometrical parameter of the lens named the bore radius R.

Keywords: Electron Microscopy, Electron and Ion optics, Objective Magnetic Lenses, Aberration.

1. Introduction

The ultimate goal of high-performance electron microscopy is the acquisition of detailed information on the atomic structure, the chemical composition and the local electronic states of real objects [1]. Any axially symmetric magnetic field produced by current-carrying coils with or without ferromagnetic materials or by permanent magnets is known as a charged particle lens (magnetic lens) [2]. An axially symmetric electric or magnetic field can be used to focus a beam of electrons much as a light lens focuses visible rays. Electric or magnetic field that are axially symmetry, or a combination of the two, acts in a similar manner on the trajectories of electrons traveling through the field. Electrons that enter the field along paths close to the axis and nearly parallel to the axis experience a radial force which is proportional to the distance of electrons from the axis. The electron trajectories therefore, are deflected in proportional to their distance from axis, and the axially symmetric field acts as a lens. Figure1 illustrates an electric electron lens and a magnetic electron lens, respectively [3].

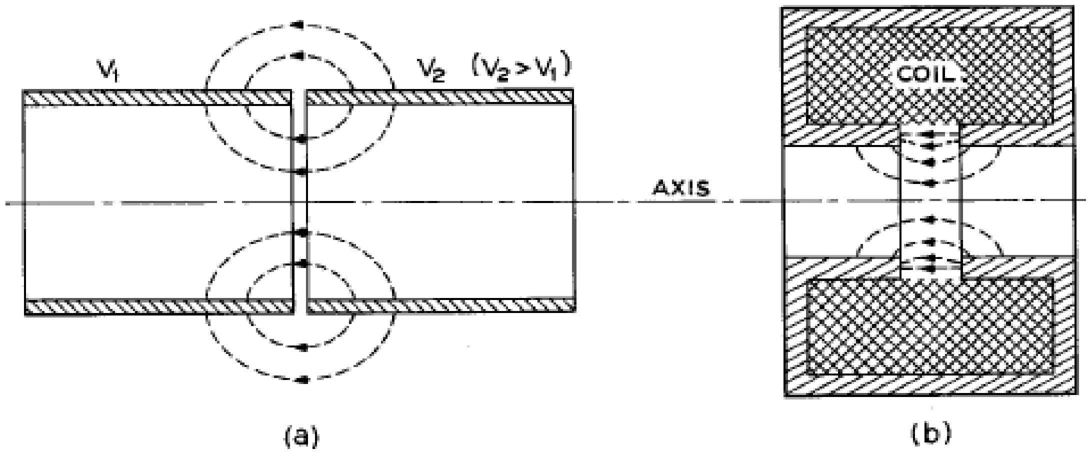

Figure 1. Type of lens: (a) an electric electron lens and, (b) a magnetic electron lens [3].

The vast majority of focusing elements used in electron and ion optics consists of axially symmetric electrostatic and/or magnetic fields that can represented by scalar potential functions [2]. Generally, electric and magnetic scalar potential distributions in electron optical devices are determined numerically with aid of some specific numerical methods such as the finite element method (FEM) or the finite difference method (FDM); see [4]. However, those may determine using some analytical target axial functions, see [5-6]. Hence, in the present article the latter procedure has been followed, where the axial magnetic scalar potential distribution of the magnetic lens has been evaluated using a convenience suggested target function in the domain of the optical axis of the lens under consideration.

2. Mathematical Remediation

The potential at distance r from the axis of an axially symmetric potential distribution is given in terms of the potential along the axis by [7],

$$V(r,z) = V(0,z) - \frac{r^2}{4} V''(0,z) + \frac{r^4}{64} V''''(0,z) - \ldots.. \quad (1)$$

where V(0,z)=V(z) is the potential along the axis, and the primes indicate differentiation with respect to z [1]. By means of equation (1) the potential at all points in an axially symmetric potential region can be described in terms of the potential on the axis. For regions close to the axis we can neglect all higher order terms and take only the first two terms of this expression, so that the potential distribution in the meridional plane (r, z), can be determined as follows.

$$V(r,z) = V(0,z) - \frac{r^2}{4} V''(0,z) \quad (2)$$

However, in the present work the following target function has been used to determine the axial magnetic scalar potential distribution V(z) of the magnetic lens,

$$V(z) = \frac{1}{2}\left[(V_1 + V_2) + (V_2 - V_1)\tanh\left(\frac{1.32z}{R}\right)\right] \quad (3)$$

IOP Conf. Series: Journal of Physics: Conf. Series **1003** (2018) 012111 doi:10.1088/1742-6596/1003/1/012111

where V_1 and V_2 represents the potential values at terminals of the lens, i.e., $V_1=V_s$ and $V_2=V_f$, and R represents the pole piece radius. By using the equation [$\mathbf{B}=-\mu_o \mathbf{grad} V$] the axial component of the magnetic field can be determined as follows,

$$B_z(z) = -\mu_o \frac{dV(z)}{dz} \tag{4}$$

where μ_o is the magnetic permeability in vacuum (4π x10^{-7} Hm^{-1}). Hence, by differentiating equation (3) by means of equation (4), one can get the axial magnetic field distribution component given by,

$$B_z(z) = \mu_o \left(\frac{V_2 - V_1}{2}\right)\left(\frac{1.32}{R}\right) sech^2\left(\frac{1.32z}{R}\right) \tag{5}$$

it is easy then to use equation (5) to assigning the imaging magnetic field distribution $B_z(z)$ along the optical axis $z_s \le z \le z_f$. Once the magnetic field is determined, the next step is to calculate the electron beam trajectory r(z) and its correspondence departure r'(z) along the axis of the lens. Typically, this task can be achieved by solving the paraxial ray equation given by the following ordinary second order differential equation [8],

$$r'' + \frac{\eta}{8V_r} B_z^2(z) r = 0 \tag{6}$$

where η is the mass m to the charge e ratio of the electron, and V_r is defined as the corrected relativistically accelerating voltage which is given by [9],

$$V_r = V_a\left(1 + \frac{eV_a}{2mc^2}\right) = V_a\left(1 + 0.978x10^{-6} V_a\right) \tag{7}$$

where V_a is the applied accelerating voltage. It is well known that the distinctive feature of magnetic lenses is that their optical properties are dependent on the charge to mass ratio of the particles [2]. To obtain the electron beam trajectory inside the electron optical device (the magnetic lens in the present work) the paraxial ray equation (6) can be solved analytically or numerically according to the constraints imposed in the study. However, the forth-order Runge-Kutta method has been used to solve the trajectory equation numerically in terms of the field distribution under zero magnification mode. A ''weak'' lens is one for which the focal length is long compared with the region of field. Suppose that an electron approaches such a lens along a path that is initially parallel to the axis but displaced a small distance from it. Equation (6) can be integration along the axis between points on either side of the lens where the field is zero, we obtain [3],

$$r'_f = -\frac{\eta}{8V_r} \int_{z_s}^{z_f} B_z^2(z) r dz \tag{8}$$

where z_s and z_f are points on the axis on opposite sides of the lens and beyond the region of field, and r'_f is the slope of the trajectory at $z=z_f$. If the focal length is long compared with the region of field, r will remain nearly constant in the region of field and can be taken outside the integral in equation (8). The focal length f_o for such a lens is then given by [3],

$$\frac{1}{f_o} = -\frac{r'_f}{r} = \frac{\eta}{8V_r} \int_{z_s}^{z_f} B_z^2(z) dz \tag{9}$$

The axial magnetic flux density would be proportional to the gradient of this is given by equation (5), then substituting this equation in equation (9), we obtain for the reciprocal of the focal length,

$$\frac{1}{f_o} = \frac{\eta\mu_o^2}{8V_r}\left(\frac{V_2 - V_1}{2}\right)^2\left(\frac{1.32}{R}\right)^2\int_{z_s}^{z_f} sech^4\left(\frac{1.32z}{R}\right)dz \tag{10}$$

using the relations [$sech^2z=1-tanh^2z$] and [$sech^2zdz=d(\tanh z)$], we obtain,

$$\frac{1}{f_o} = \frac{\eta\mu_o^2}{8V_r}\left(\frac{V_2 - V_1}{2}\right)^2\left(\frac{1.32}{R}\right)^2\left(\frac{R}{1.32}\right)\left[tanh\left(\frac{1.32z}{R}\right) - \frac{tanh^3}{3}\left(\frac{1.32z}{R}\right)\right]_{z_s}^{z_f} \tag{11}$$

$$\frac{1}{f_o} = \frac{\eta\mu_o^2}{8V_r}\left(\frac{V_2 - V_1}{2}\right)^2\left(\frac{1.32}{R}\right)^2\left(\frac{R}{1.32}\right)\left(\frac{4}{3}\right) \approx \frac{\eta R\mu_o^2}{8V_r}\left(\frac{V_2 - V_1}{2}\right)^2\left(\frac{1.32}{R}\right)^2 \tag{12}$$

where the points z_s and z_f have been taken to be effectively at ($-\infty$ and $+\infty$), respectively. The focal length f_o is therefore given by,

$$f_o = \frac{8V_r}{\eta R\mu_o^2\left(\frac{V_2 - V_1}{2}\right)^2\left(\frac{1.32}{R}\right)^2} \tag{13}$$

If an electron trajectory after emerging on one side of a lens lies in a plane containing the axis, the trajectory after emerging from the lens will also lie in a plane containing the axis. However, the second plane is rotated about the axis from the first plane. The angle of rotation between the planes is given by [3],

$$\theta = \frac{\eta}{2}\int_{t_1}^{t_2} B_z dt = \frac{\eta}{2}\int_{z_s}^{z_f} B_z \frac{dz}{dz/dt} = \sqrt{\frac{\eta}{8V_r}}\int_{z_s}^{z_f} B_z(z)dz \tag{14}$$

where t_1 and t_2 are, respectively, the times at which the z coordinate of the electron is z_s and z_f, and where it is assumed that $\dot{z}$ (dz/dt) is very nearly constant through the lens and is equal to $(2\eta V_r)^{1/2}$. If $B_z(z)$ is in the direction of travel of the electron, Θ is positive, then by substituting equation (5) in equation (14), we obtain the angle of rotation of electron along the terminals $z=z_s$ to $z=z_s$ as follows,

$$\theta = -\mu_o\sqrt{\frac{\eta}{8V_r}}\left(\frac{V_2 - V_1}{2}\right)\left(\frac{1.32}{R}\right)\int_{z_s}^{z_f} \sec h^2\left(\frac{1.32z}{R}\right)dz$$

$$\theta = -\mu_o\sqrt{\frac{\eta}{8V_r}}\left(\frac{V_2 - V_1}{2}\right)\left(\frac{1.32}{R}\right)\left(\frac{R}{1.32}\right)tanh\left(\frac{1.32z}{R}\right)$$

$$\theta = -\mu_o\left(\frac{V_2 - V_1}{2}\right)\sqrt{\frac{\eta}{8V_r}}tanh\left(\frac{1.32z}{R}\right) \tag{15}$$

The final task of the synthesis approach is finding the profile of the electrode or pole piece of the electron optical device, however, equation (2) may be used to obtain the shape of the pole piece that produce the field distribution as follows [10-11],

$$R_P(z) = 2\sqrt{\frac{V(z) - V_P}{V''(z)}} \tag{16}$$

where R_p is the radial height of the pole piece, V_P is the potential value at the pole piece surface, which is equivalent to half of the lens excitation NI in the case of symmetrical charged particle lens, and $V''(z)$ is the second derivative of the magnetic scalar potential V(z) which can be obtained from equation (3) as follows with aid of Simpson rule numerical method.

$$V''(z) = -(V_2 - V_1)\left(\frac{1.32}{R}\right)^2 \tanh\left(\frac{1.32z}{R}\right)\sec h^2\left(\frac{1.32z}{R}\right) \tag{17}$$

The spherical and chromatic aberration coefficients C_s and C_c of any axially symmetric magnetic lenses can be calculated using the following integral [8],

$$C_s = \frac{\eta}{128V_r}\int_{z_o}^{z_i}\left[\left(\frac{3e}{mV_r}\right) + B_z^4(z)r_\alpha^4(z) + 8B_z'^2(z)r_\alpha^4 - 8B_z^2(z)r_\alpha^2 r_\alpha'(z)\right]dz \tag{18}$$

$$C_c = \frac{\eta}{8V_r}\int_{z_o}^{z_i} B_z^2(z)\, r_\alpha^2(z)\, dz \tag{19}$$

where $r_\alpha(z)$ is the solution of the paraxial ray equation, and primes indicate differentiation with respect to the axial coordinate z.

3. Magnetic Lens Simulation

The Simulink is a companion application to Matlab, it deals with the engineering and scientific problems in terms of complete models. The Simulink can be considered as a powerful tool to solve different problems in terms of various blocks. Simulink in Matlab include comprehensive libraries. However, each library contains different specific blocks. Each block may be correspondent to a mathematical operation, such as: the addition, subtraction, multiplication, division, or matrices operations. Also, there are some blocks represents constants, signals, integrator, derivatives, gains, and waves. The input and output of each model can be obtained by specific blocks, such as: 'From workspace', 'To workspace', 'Scope' block, and 'XY Graph' block. The Simulink produces powerful complete models in the image processing, signal processing, communications, etc. Where, there are specific blocks determining the conversion, transformation, filtering, etc. All special mathematical functions, such as: trigonometric functions, inverse trigonometric functions, hyperbolic, inverse hyperbolic, exponential, logarithmic functions can be determined with aid of special blocks. Linear and nonlinear mathematical functions as well as polynomials also can be calculated with aid of Simulink. All logic and bit operations can be executed by special blocks, for more details see [12].

In this paper we used the direct Simulink method to simulate and determine the related axial functions of the magnetic lens under consideration in terms of different Simulink models. Figure 2 shows a Simulink model aiming to create the distributions of the axial potential and axial magnetic field which is buildup on the target axial magnetic potential function and the magnetic field distribution given in equations (3) and (5) respectively.

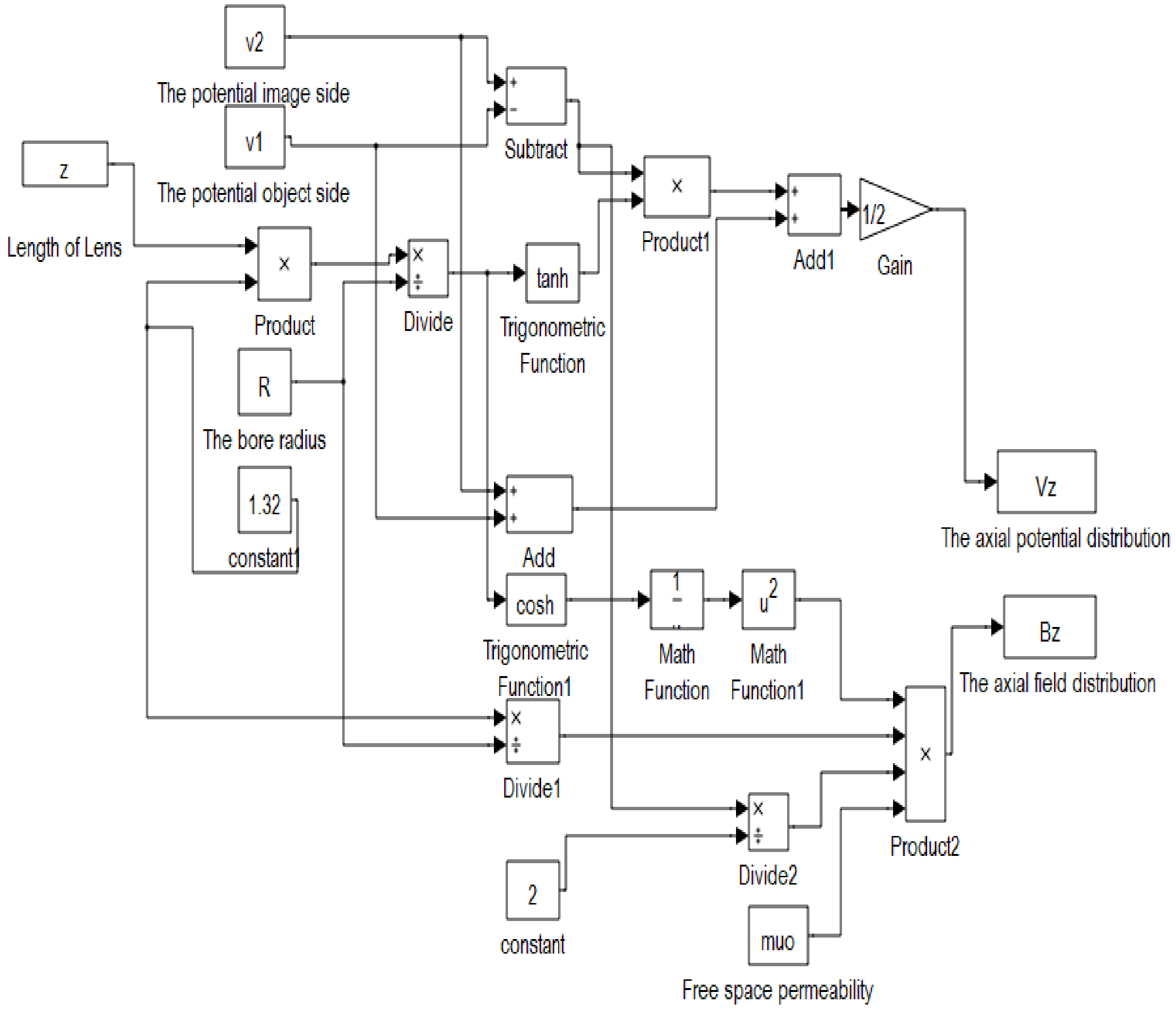

Figure 2. Simulink model for the axial magnetic scalar potential and axial field distributions.

With aid of equations (16) and (17), figure3 shows the Simulink model aiming in creation the shape of the pole piece and the distribution of the second derivative of the axial potential.

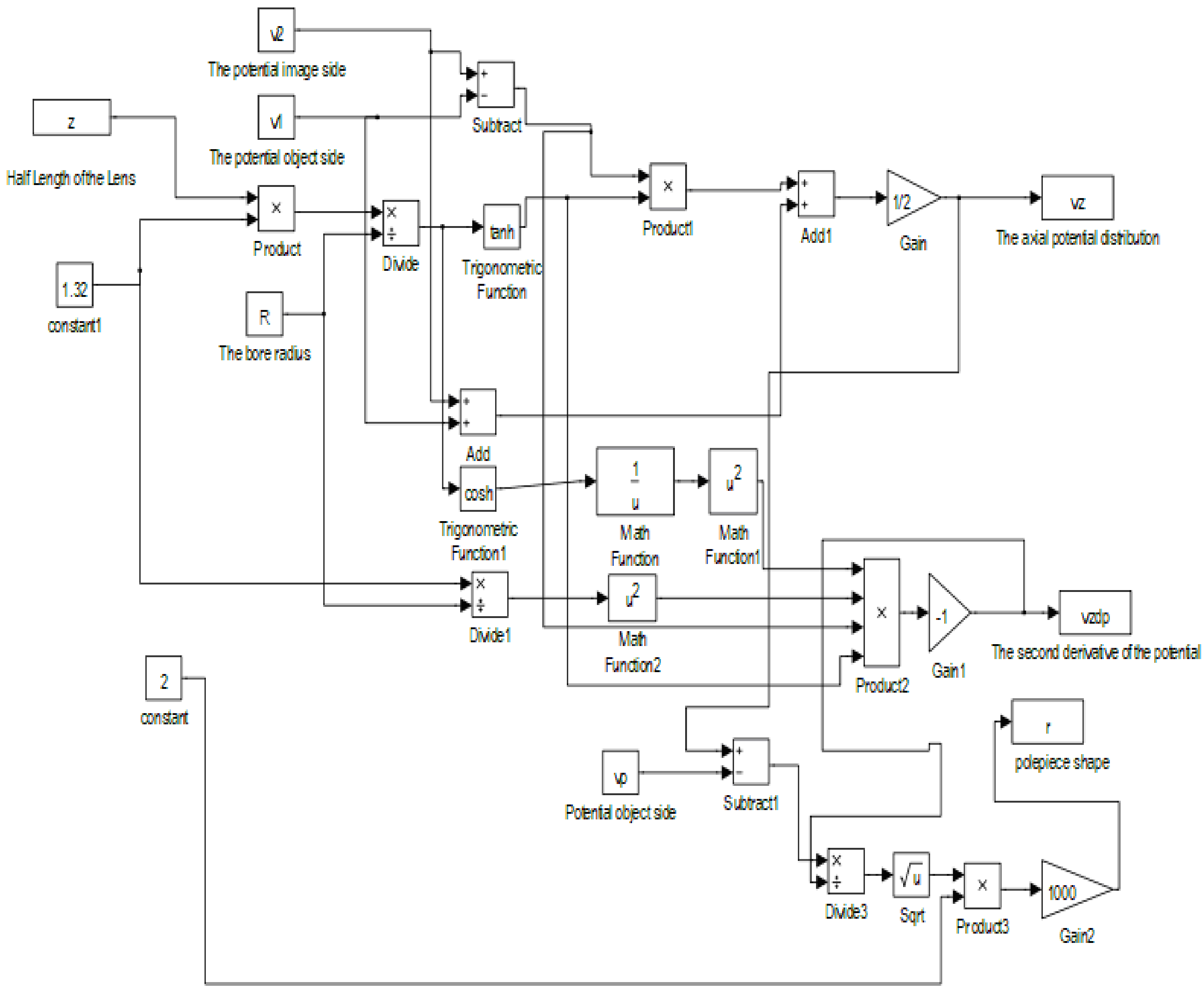

Figure 3. Simulink model for the axial magnetic scalar potential, V″(z) and pole shape.

The results of simulation in two mentioned models are the axial distributions of potential V(z), magnetic field B_z, and , V″(z) at specific input parameters as well as the shape of the pole piece plotted in 'figure 4' , 'figure 4' respectively.

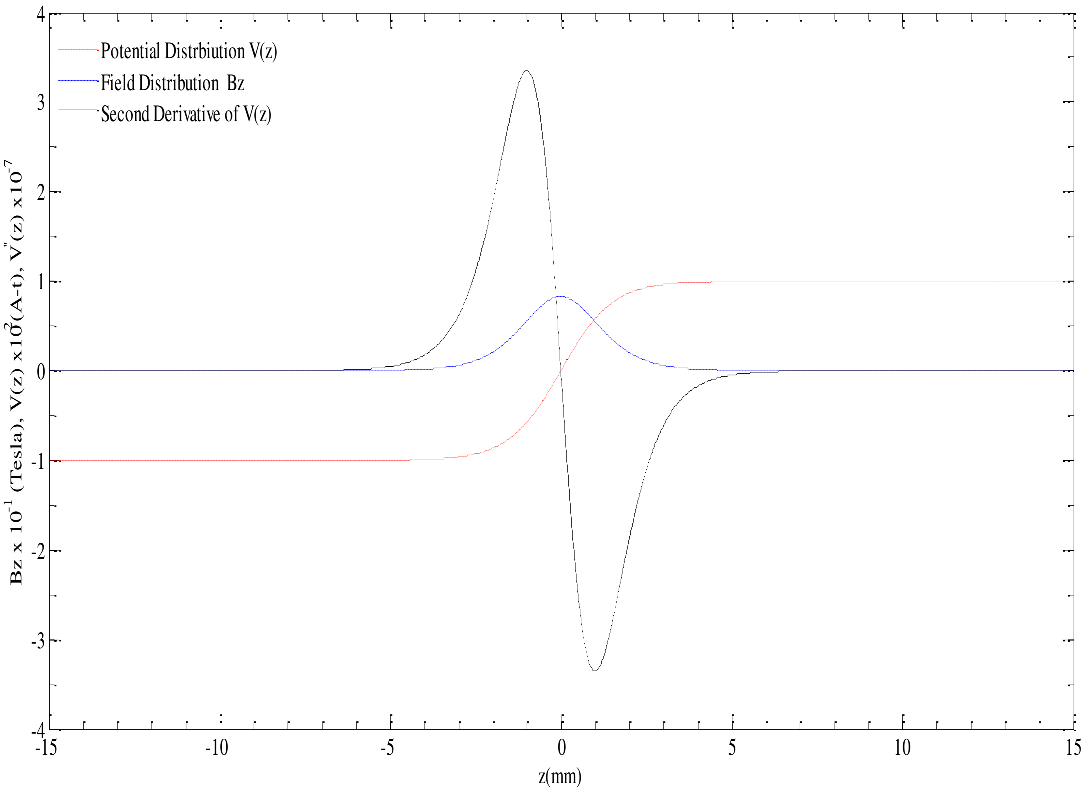

Figure 4. The axial distributions of V(z), $B_z(z)$ and V″(z) along the optical axis of the lens at V_1=V_2=-100A-t, R=2mm and L=30mm.

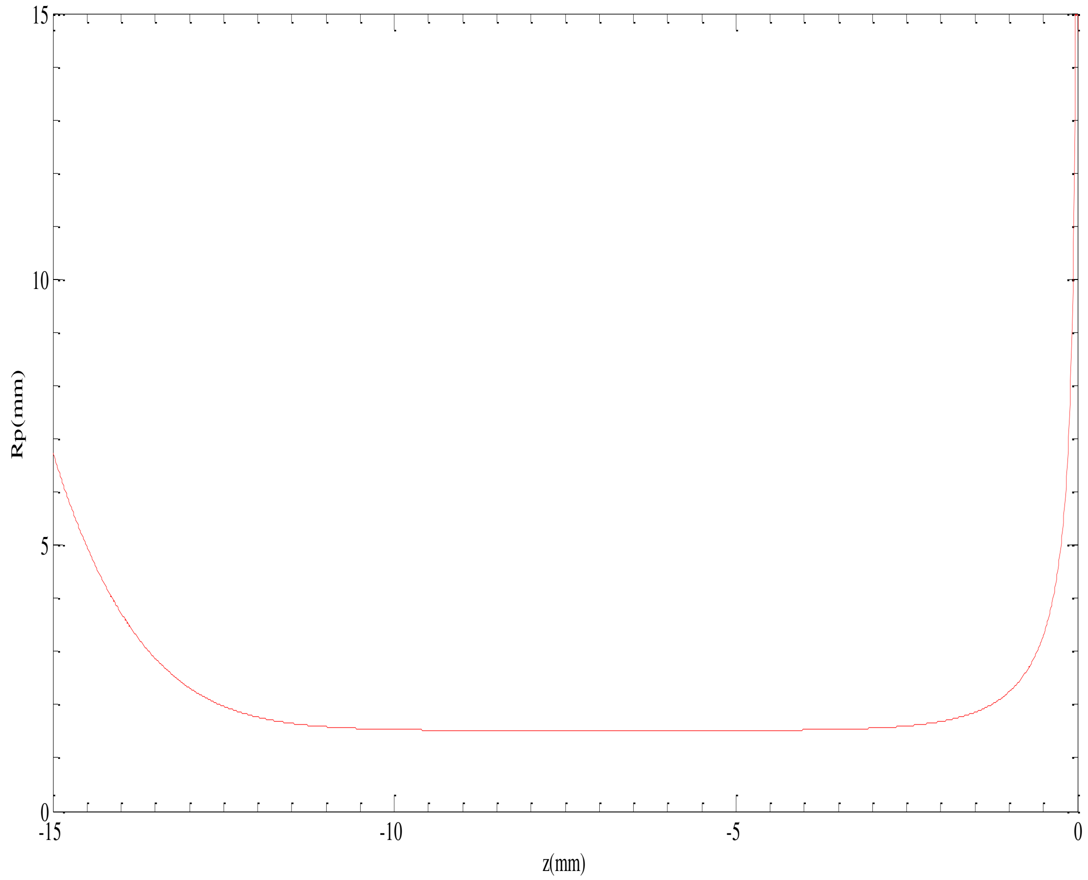

Figure 5. The profile of the magnetic pole piece at V_1=V_2=-100A-t, R=2mm and L=30mm.

4. Results and Discussion

To study the effect of the important optimization parameter in equation (3) that called pole piece radius of the lens (bore radius) R, the following five values of R are selected (1, 2, 3, 4, and 5 mm), the lens operates under the magnetic unsaturated mode, and other parameters are kept constant (the length of the lens is kept constant at 30 mm and the potentials at the terminals of the lens (i.e., at the object and image sides) are kept at V_1=-100A-t (Ampere-turn) and V_2=100A-t). Regarding the two equations (3) and (5), one can plot the magnetic scalar potential distribution and the magnetic field distribution, as shown in figures 6 and 7 where both figures are sketched for diverse values of the lens radius R. It is obvious that when the optimization parameter R is increased the peak field value B_{max} of the corresponding fields is affected and decreased. The lens excitation NI (Ampere-turn) is equal to the area under the curve of the magnetic field distribution which remains unchanged for all R values since the potential values V_1 and V_2 are kept constant. This means that the field distribution would be not more distributed along a large axial extension of the optical axis for large values of parameter R. It is noted that the magnetic scalar potential distribution curve plotted in figure 6 is affected by varying R values, so the potential gradient increases with increasing R. The magnetic pole pieces that produce the desired field distribution can be reconstructed with aid of equation (16), thus, figure 8 shows the half upper part of the double pole piece magnetic lens profile for various values of the bore radius R. Figure 9, shows the angle of rotation of electron about the optical axis of the magnetic lens, at terminals z_s to z_f for diverse values of the bore radius R, this figure plotted according to equation (15). It will be mentioned that the angle of rotation decreasing with increasing the pole piece radius R.

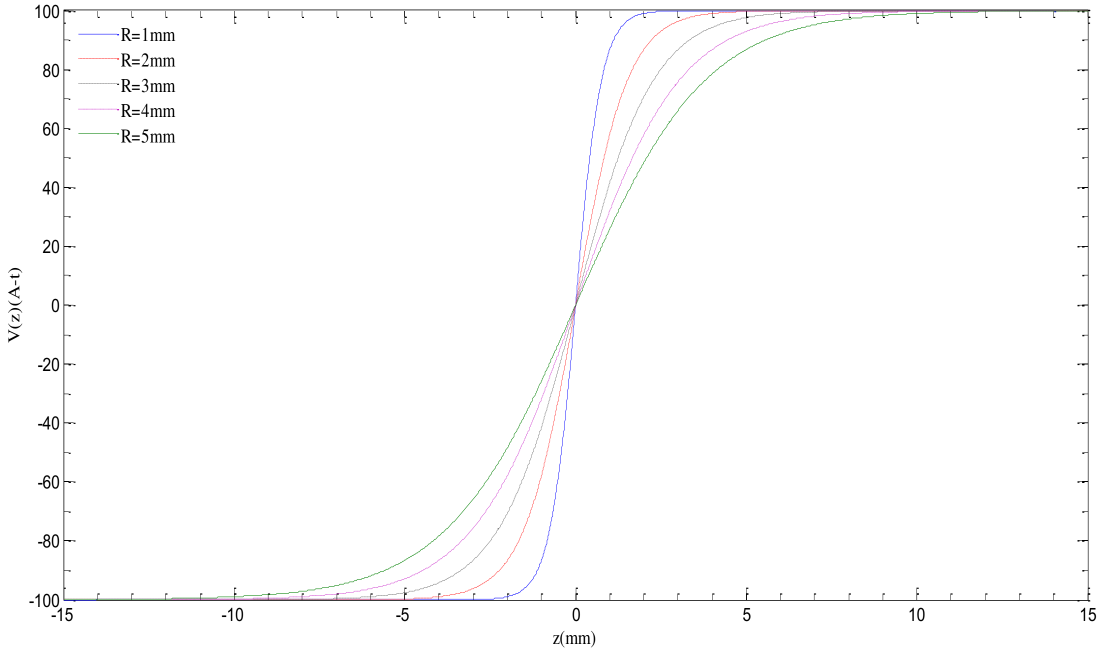

Figure 6. The axial magnetic scalar potential distribution for different values of the pole piece radius R.

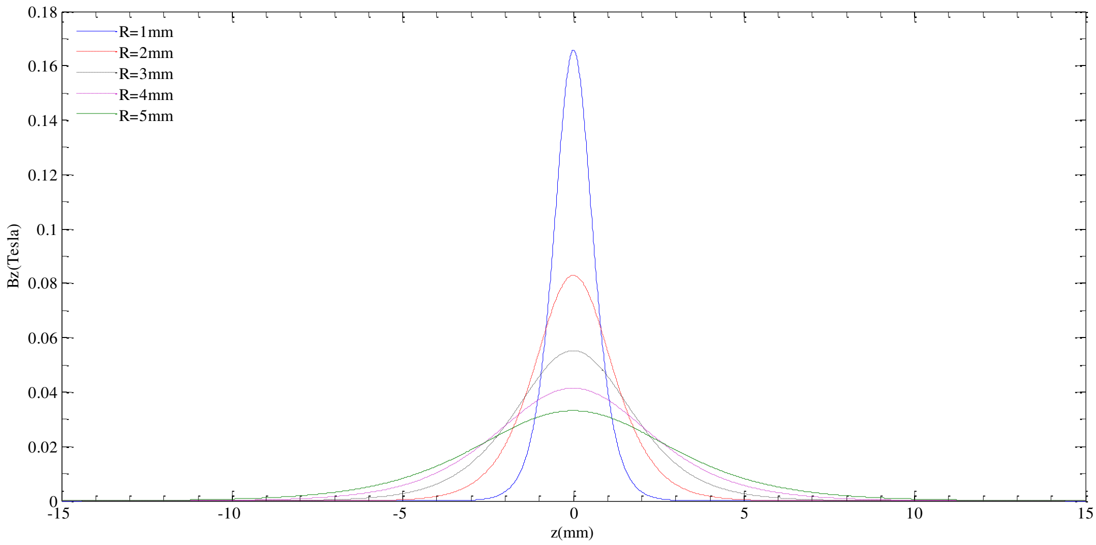

Figure 7. The axial magnetic field distribution for different values of the pole piece radius R.

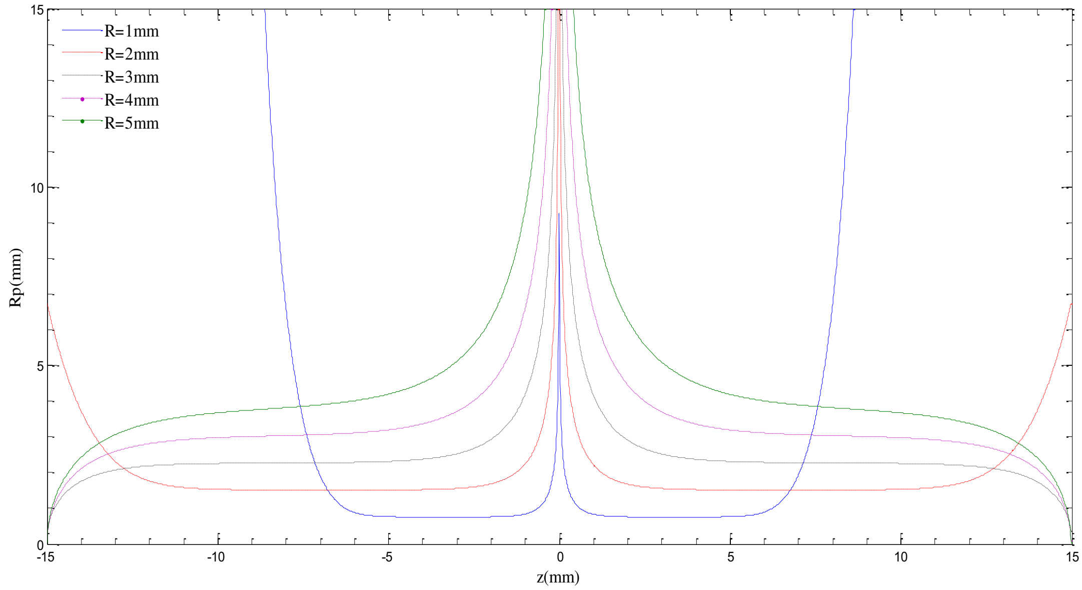

Figure 8. The half upper reconstructed magnetic pole piece shape for different values of the pole piece radius R

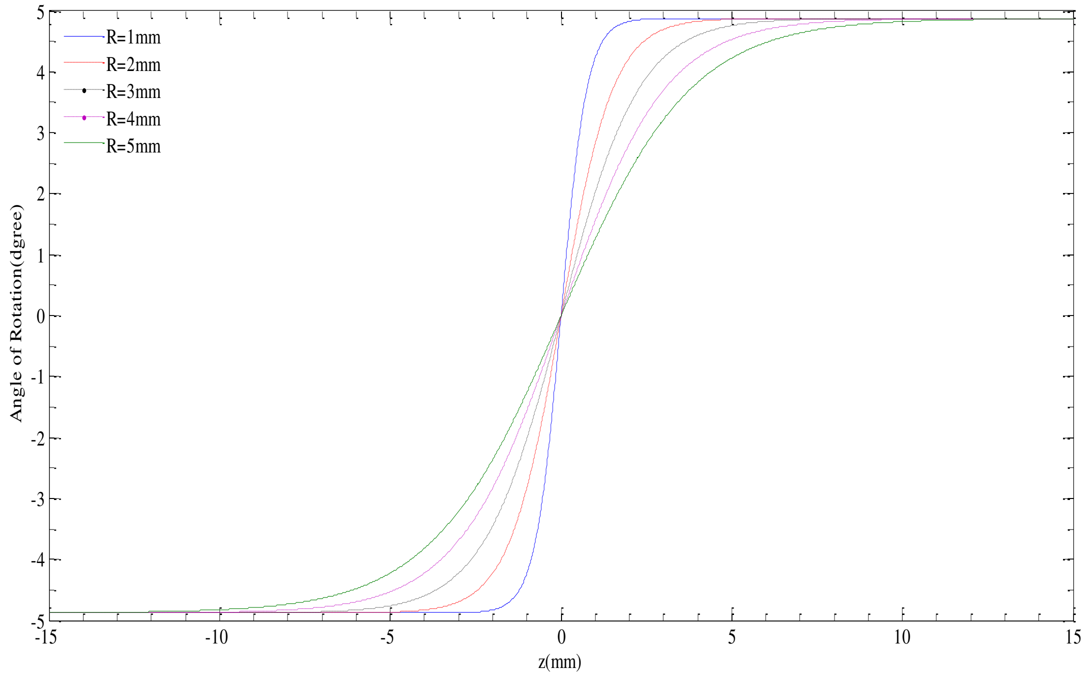

Figure 9. The angle of rotation of electron about the z-axis for different values of the pole piece radius R.

IOP Conf. Series: Journal of Physics: Conf. Series **1003** (2018) 012111 doi:10.1088/1742-6596/1003/1/012111

The important values of some design parameters are shown in Table (1). The columns in this table represent the setup values of the lens radius R, the maximum value of the magnetic field (peak values) B_{max}, the half width of the field W, and the area under the curve NI (excitation of the lens). The investigation shown that as the parameter R is increased, W also increasing, while B_{max} is decreasing, and NI remains almost constant.

Table 1. Lens design parameters for different values of pole piece radius R at V_2=-V_1=-100(A-t) and L=30mm.

R(mm)	B_{max}(T)	W(mm)	NI(A-t)
1	0.166	1.335	200
2	0.083	2.671	200
3	0.055	4.006	200
4	0.042	5.342	200
5	0.033	6.677	200

Table 2 shows the objective optical properties, the columns in this table represent the setup values of the lens radius R, the objective focal length f_o computed from the program and equation (13), the spherical aberration coefficient C_s and the chromatic aberration coefficient C_c. It will be noted from the Table 2 that all the optical properties are increasing with increasing R, with convergence in values between two focal lengths that are computed from the program and equation (13), which means that the objective optical properties of the objective magnetic lens affected and become worst by increasing the lens radius (bore radius) R.

Table 2. Optical objective properties for different values of pole piece radius R at V_2=V_1=-100(A-t) and L=30mm at NI/$Vr^{1/2}$=20.

R(mm)	f_o(mm) from the program	f_o(mm) from the equation (13)	C_s(mm)	C_c(mm)
1	0.514	0.408	0.248	0.356
2	1.027	0.816	0.498	0.712
3	1.540	1.224	0.748	1.068
4	2.054	1.632	0.998	1.423
5	2.566	2.040	1.247	1.778

5. Conclusions

In accordance with the aspects and results illustrated in the present work, several conclusions could be written down. However, the most important remarks can be summarized as follows;

1. The study showed that the optical properties have been worse when increasing the bore radius of the lens.
2. The study also showed that the area under the curve (excitation of the lens) and corrected relativistically, accelerating voltage remains nearly constant at different values of the radius of the lens.

References

[1] Rose H and Wan W 2005 Aberration correction in electron microscopy proceeding of particle Acce elerator conference, Knoxville,Tennessee, LBNI Berkeley, CA94720, USA, pp **44-48**

[2] Szilagyi M 1988 Electron and ion optics Plenum Press New York and London

IOP Conf. Series: Journal of Physics: Conf. Series **1003** (2018) 012111 doi:10.1088/1742-6596/1003/1/012111

[3] Klempere O 1953 Electron Optics,2nd Edition Cambridge University Press, Cambridge, England
[4] Munro M 1971 Computer- Aided Design Methods in Electron optics Ph.D. Thesis, University of Cambridge, UK.
[5] Al-Batat A H H '2013 Modeling and Design For Objective Charged *Particle Lens Journal of (IJAIE M),* vol **2,** Issue **10**, pp **25-32**
[6] A. H. H.Al-Batat A H H, Yaseen M J and Majeed M M 2011 Investigation of the projector Properties of the magnetic lenses using analy-tical function *Ibn Al-Haithom journal for pure and applied science*, vol **24**, No.**1** pp **63-71**
[7] Szilagyi M 1984 Reconstruction of Electrodes and Pole pieces from Optimized Axial Field Distributions of Electron and Ion Optical Systems *Appl. Phys. Lett.,* **45**, pp **499-501**
[8] El-Kareh A B and El-Kareh J C J 1970 Electron beams, lenses, and optics vol**2**, p**49,**(New York Academic)
[9] Klemprer O 1971Electron Optics **3**rd ed., (Cambridge)
[10] Szilagyi, M. 1985 Electron optical synthesis and optimization Proceeding of the IEEE, **73**, No. **3**
[11] Al. Batat A H H, Hasan H S, *Ibrahim Husin H M and Yaseen M J* 2016 Modulating Mathematical Function to be used in Electron Objective *Lens Journal of Advances in Physics Theories and Applications,* vol **57**, pp.**8-15**
[12] Karris T 2006 Introduction to Simulink with e